European Journal of Medicinal Chemistry 183 (2019) 111717

Contents lists available at ScienceDirect

European Journal of Medicinal Chemistry

journal homepage: http://www.elsevier.com/locate/ejmech

Research paper

Design, synthesis and biological evaluation of *N*-(3-(1*H*-tetrazol-1-yl) phenyl)isonicotinamide derivatives as novel xanthine oxidase inhibitors

Ting-jian Zhang, Yi Zhang [1], Shun Tu [1], Yu-hang Wu, Zhen-hao Zhang, Fan-hao Meng*

School of Pharmacy, China Medical University, 77 Puhe Road, North New Area, Shenyang, 110122, China

ARTICLE INFO

Article history:
Received 12 July 2019
Received in revised form
6 September 2019
Accepted 17 September 2019
Available online 18 September 2019

Keywords:
Xanthine oxidase inhibitor
Isonicotinamide
Structure-based drug design
Hyperuricemia

ABSTRACT

In our previous study, we reported a series of *N*-phenylisonicotinamide derivatives as novel xanthine oxidase (XO) inhibitors and identified *N*-(3-cyano-4-((2-cyanobenzyl)oxy)phenyl)isonicotinamide (compound **1**) as the most potent one with an IC_{50} value of 0.312 μM. To further optimize the structure and improve the potency, a structure-based drug design (SBDD) strategy was performed to construct the missing H-bond between the small molecule and the Asn768 residue of XO. We introduced a tetrazole moiety at the 3′-position of the phenyl to serve as an H-bond acceptor and obtained a series of *N*-(3-(1*H*-tetrazol-1-yl)phenyl)isonicotinamide derivatives (**2a-t** and **6**–**8**). Besides, to investigate the influence of the amide-reversal, some *N*-(pyridin-4-yl)-3-(1*H*-tetrazol-1-yl)benzamide derivatives (**3c**, **3e**, **3i**, **3k** and **3u**) were also synthesized and evaluated. Biological evaluation and structure-activity relationship analysis demonstrated that the 3′-(1*H*-tetrazol-1-yl) moiety was an excellent fragment for the *N*-phenylisonicotinamide scaffold; a substituted benzyloxy, especially, an *m*-cyanobenzyloxy (*e.g.*, **2s**), linking at the 4′-position was welcome for the potency; and the amide-reversal could damage the potency, so maintenance of the *N*-phenylisonicotinamide scaffold was essential. In summary, starting from compound **1**, the SBDD effort successfully identified a promising XO inhibitor **2s** ($IC_{50} = 0.031$ μM), with a 10-fold gain in potency. Its potency was very close to the positive control topiroxostat ($IC_{50} = 0.021$ μM). A Lineweaver-Burk plot indicated that compound **2s** acted as a mixed-type XO inhibitor. Molecular docking and molecular dynamics simulations revealed that the tetrazole moiety could occupy the Asn768-subpocket with N-4 atom accepting an H-bond from the Asn768 residue, as expected.

1. Introduction

Xanthine oxidase (XO) is a key enzyme responsible for the catabolism of purines, which catalyzes the hydroxylation of both hypoxanthine and xanthine in the last two steps of urate biosynthesis in humans [1,2]. In parallel with the hydroxylation, XO transfers the electrons to oxygen molecules to form either hydrogen peroxide or superoxide anion [1,3,4]. Therefore, inhibition of XO not only effectively reduces the production of uric acid for the treatment of hyperuricemia and gout, but also benefits the pathological conditions caused by the XO-derived reactive oxygen species such as oxidative damage, post-ischemic reperfusion injury, diabetes and chronic heart failure [2,5,6].

So far, the clinically used XO inhibitors mainly include allopurinol, febuxostat and topiroxostat (Fig. 1). Allopurinol is a hypoxanthine isomer, which has been prescribed in the treatment of hyperuricemia and gout for several decades. However, it is restrained from clinical application due to serious adverse effects that possibly derived from the purine backbone [7]. Topiroxostat and Febuxostat are novel non-purine XO inhibitors basing on characteristic five-membered ring linkers with high in vitro enzyme inhibitory activity in the nanomolar level. Both of them have been approved by the U.S. Food and Drug Administration (FDA). However, some side effects were observed after the clinical application. Topiroxostat may enhance the incidence of gouty arthritis [8]. And on February 21, 2019, FDA had concluded there is an increased risk of heart-related death with febuxostat (Uloric) compared to allopurinol. Hence, it is an urgent requirement to discover novel XO inhibitors having fewer adverse effects in the

* Corresponding author.
E-mail address: fhmeng@cmu.edu.cn (F.-h. Meng).
[1] These two authors contributed equally to this work.

https://doi.org/10.1016/j.ejmech.2019.111717
0223-5234/

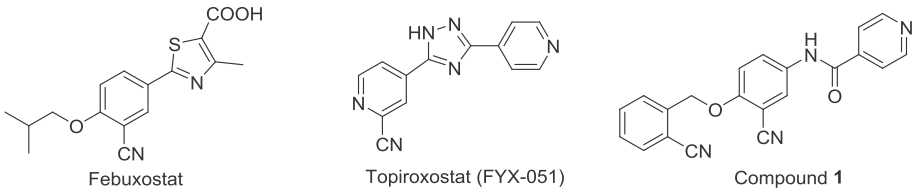

Fig. 1. Chemical structures of febuxostat, topiroxostat and compound **1**.

treatment of gout and related complications. In addition, numerous XO inhibitors have been reported in recent years including isocytosines [9–12], pyrano[3,2-d]pyrimidines [13], pyrazoles [14], thiazoles [15], 2-mercapto-6phenylpyrimidine-4-carboxylic acids [16], 2-arylbenzo[b]furans [17,18], flavonoids [19–22], chalcones [23], fraxamosides [24], etc.

In the past few years, our team has been working on the discovery of novel XO inhibitors. We successively reported multiple series of XO inhibitors based on the diverse scaffolds [25–28]. With these experiences, we employed an amide fragment as an opened-ring isostere of five-membered ring linkers of classic XO inhibitors (*e.g.*, 1,2,4-triazole in topiroxostat and thiazole in febuxostat) to give a kind of novel scaffold basing on an *N*-phenylisonicotinamide for the first time, and identified a potent XO inhibitor *N*-(3-cyano-4-((2-cyanobenzyl)oxy)phenyl)isonicotinamide (compound **1**, Fig. 1) [29]. The molecular docking studies indicated that compound **1** could form a set of interactions with XO active pocket [29]. However, a crucial H-bond interaction linking to the terminal amino of Asn768 residue was missing [30–32]. Since the terminal amino of Asn768 usually acts as an H-bond donor during the interaction, the absence of the corresponding H-bond acceptor on compound **1** is very likely the main cause of a significant decrease in potency compared with topiroxostat.

To further optimize the structure of *N*-phenylisonicotinamide and to improve the XO inhibitory potency, structure-based drug design (SBDD) was carried out. The Asn768 residue is located at a sub-pocket (marked as Asn768-sub-pocket) that is large enough to accommodate a flat five-membered ring [31,33]. Tetrazole is a popular drug-like fragment that has been widely used by medicinal chemists in drug design [34–36]. Considering that each N atom of the tetrazole has the potential to serve as an H-bond acceptor, tetrazole is a good choice to match the Asn768-sub-pocket. Therefore, we employed a tetrazole moiety to link at the 3′-position of the phenyl to obtain a series of *N*-(3-(1*H*-tetrazol-1-yl)phenyl) isonicotinamide derivatives (**2a-t** and **6**–**8**), hoping that, the larger size tetrazole could occupy the Asn768-sub-pocket, approach Asn768 residue from more potential angles and interact with it. Furthermore, to investigate the influence of the amide-reversal, some *N*-(pyridin-4-yl)-3-(1*H*-tetrazol-1-yl)benzamide derivatives (**3c**, **3e**, **3i**, **3k** and **3u**) were also synthesized and evaluated. Also, steady-state kinetic analysis and molecular modeling studies were performed to investigate the inhibition behaviors of the optimized compound.

2. Results and discussion

2.1. Chemistry

The synthesis of *N*-(4-alkoxy-3-(1*H*-tetrazol-1-yl)phenyl)isonicotinamides (**2a-t** and **6**–**8**) was performed as outlined in Scheme l. Commercially available 2-amino-4-nitrophenol was reacted with NaN_3 and triethyl orthoformate to obtain 4-nitro-2-(1*H*-tetrazol-1-yl)phenol (**4**). The reduction of **4** by iron powder in the presence of ammonium chloride yielded 4-amino-2-(1*H*-tetrazol-1-yl)phenol (**5**), which was alkylated with isonicotinoyl chloride in the presence of triethylamine to provide di-isonicotinoyl product (**6**). The extra isonicotinoyl linking on the hydroxyl group was removed in a sodium hydroxide aqueous solution to provide key intermediate *N*-(4-hydroxy-3-(1*H*-tetrazol-1-yl)phenyl)isonicotinamide (**7**). Acetylation of compound **7** with

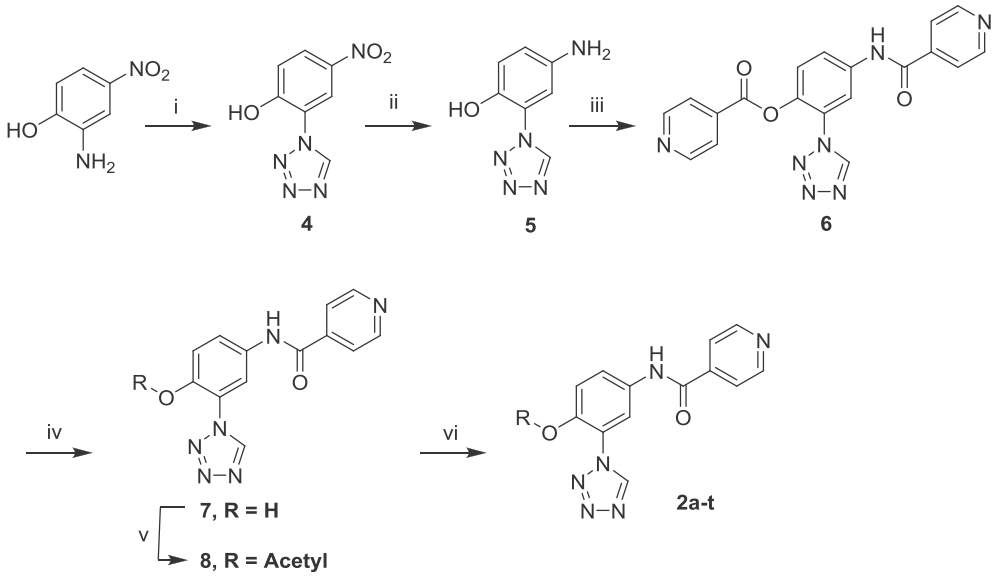

Scheme 1. Reagents and conditions: (i) NaN_3, triethyl orthoformate, AcOH, 80 °C, overnight; (ii) Fe, NH_4Cl, EtOH, H_2O, 80 °C, overnight; (iii) isonicotinoyl chloride, Et_3N, DCM, −5 °C, 1 h; (iv) NaOH, MeOH, H_2O, 50 °C, 4 h; (v) Acetyl chloride, Et_3N, THF, overnight; (vi) RCl or RBr, K_2CO_3, KI, DMF, 60 °C for 3 h, or 25 °C for 48 h.

acetyl chloride gave compound **8**, and alkylation of compound **7** with various alkyl chlorides or alkyl bromides obtained *N*-(4-alkoxy-3-(1*H*-tetrazol-1-yl)phenyl)isonicotinamides (**2a-t**).

The synthesis of 4-alkoxy-*N*-(pyridin-4-yl)-3-(1*H*-tetrazol-1-yl) benzamides (**3c**, **3e**, **3i**, **3k** and **3u**) was carried out by a similar procedure as shown in Scheme 2. Commercially available 3-amino-4-hydroxybenzoic acid was treated with NaN_3 and triethyl orthoformate to yield 4-hydroxy-3-(1*H*-tetrazol-1-yl)benzoic acid (**9**). Compound **9** was alkylated with various alkyl chlorides or alkyl bromides, and followed by a hydrolysis reaction to provide key intermediates 4-alkoxy-3-(1*H*-tetrazol-1-yl)benzoic acids (**11**). Compounds **11** were treated with thionyl chloride to yield 4-alkoxy-3-(1*H*-tetrazol-1-yl)benzoyl chloride hydrochlorides (**12**). The Acylation of pyridin-4-amine with compounds **12** in the presence of triethylamine provided target compounds 4-alkoxy-*N*-(pyridin-4-yl)-3-(1*H*-tetrazol-1-yl)benzamides **3c**, **3e**, **3i**, **3k** and **3u**.

The structures were elucidated by HRMS, ^{1}H NMR, and ^{13}C NMR spectra. All spectral data were in accordance with the assumed structures. In ESI-HRMS analysis, the target compounds showed $[M-H]^-$ ion peaks. In ^{1}H NMR spectra, the CH of tetrazole and the NH of amide were observed at approximately 9.80 ppm and 10.67 ppm, respectively.

2.2. Biological activity

The in vitro bovine XO inhibitory activity of compounds **2a**–**t**, **3c**, **3e**, **3i**, **3k**, **3u** and **6**–**8** was measured spectrophotometrically by determining uric acid production at 294 nm. Topiroxostat and compound **1** were included as reference compounds. The testing results are shown in Table 1 and Table 2.

As shown in Table 1, most of the compounds presented much higher potency than compound **1**, revealed that tetrazole fragment was greatly beneficial for the XO inhibitory potency, and introduction of the tetrazole moiety at the 3′-position was a successful optimization strategy. However, the amide-reversal didn't achieve positive results. As displayed in Table 2, all the amide-reversal derivatives (**3c**, **3e**, **3i**, **3k** and **3u**) displayed poor activities, which were 18–30 times lower than their *N*-phenylisonicotinamide counterparts. Therefore, the *N*-phenylisonicotinamide scaffold should be maintained, and our efforts were mainly focused on the *N*-phenylisonicotinamide series.

Numerous studies have proven that the substituent near the

Table 1
In vitro XO inhibitory potency of compounds.

Compounds	R groups	IC_{50} (μM)[a]
2a	*iso*-Propyl	0.603 ± 0.053
2b	*n*-Butyl	0.264 ± 0.022
2c	*iso*-Butyl	0.165 ± 0.0.12
2d	*sec*-Butyl	0.171 ± 0.009
2e	*n*-Pentyl	0.174 ± 0.014
2f	*iso*-Pentyl	0.145 ± 0.012
2g	*cyclo*-Pentyl	0.128 ± 0.018
2h	Pentan-3-yl	0.141 ± 0.013
2i	*n*-Hexyl	0.153 ± 0.009
2j	*n*-Octyl	0.092 ± 0.008
2k	Benzyl	0.094 ± 0.010
2l	*o*-Methylbenzyl	0.053 ± 0.008[c]
2m	*m*-Methylbenzyl	0.044 ± 0.009[c]
2n	*p*-Methylbenzyl	0.132 ± 0.012
2o	*o*-Methoxybenzyl	0.117 ± 0.011
2p	*m*-Methoxybenzyl	0.050 ± 0.007[c]
2q	*p*-Methoxybenzyl	0.067 ± 0.009
2r	*o*-Cyanobenzyl	0.110 ± 0.014
2s	*m*-Cyanobenzyl	0.031 ± 0.004[c]
2t	*p*-Cyanobenzyl	0.100 ± 0.009
6	Isonicotinoyl	n.a.[b]
7	H	n.a.
8	Acetyl	0.173 ± 0.016
1	/	0.312 ± 0.021
Topiroxostat	/	0.021 ± 0.003

[a] Values are means ± SD of three independent experiments.
[b] n.a.: not active (<60% inhibition at 10 μM).
[c] $P < 0.05$, versus topiroxostat.

similar position of the 4′-OR group has a significant effect on potency, and the optimal substituent will change with the structure of the scaffold [37–41]. As shown in Table 1, the 4′-alkoxy and 4′-benzyloxy derivatives (**2a-t)** presented well to excellent XO inhibitory potency with IC_{50} values ranging from 0.031 to 0.603 μM. Removal of the alkyl or benzyl R group gave compound **7** accompanied by the disappearance of the potency, meaning that the lipophilic R group played a crucial role in potency. In addition, the isonicotinoyloxy derivative **6** and acetoxy derivative **8** showed poor potency as well, compound **6** was totally inactive and compound **8** presented a weak potency with an IC_{50} value of 0.17 μM, indicated that acyloxy wasn't a suitable choice for the 4′-position.

Among the 4′-alkoxy derivatives (**2a-j)**, it was found that as the size of R group increased; the potency is gradually enhanced. A similar trend was also observed in our previous works involving a

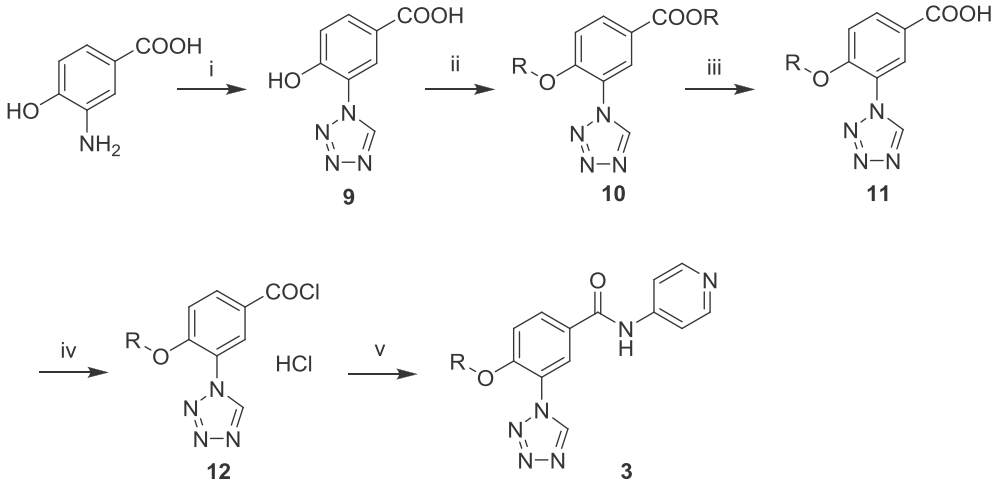

Scheme 2. Reagents and conditions: (i) NaN_3, triethyl orthoformate, AcOH, 80 °C, overnight; (ii) RCl or RBr, K_2CO_3, KI, DMF, 60 °C, 6 h; (iii) NaOH, MeOH, H_2O, 50 °C, 30 min; (iv) $SOCl_2$, DMF, 50 °C, 5 h; (v) pyridin-4-amine, Et_3N, THF, −10 °C, 1 h, then room temperature overnight.

Table 2
In vitro XO inhibitory potency of target compounds **3c**, **3e**, **3i**, **3k** and **3u**.

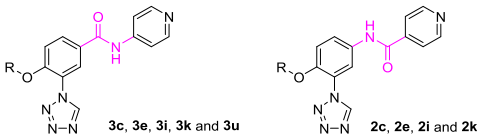

R groups	Compounds	IC_{50} (μM)[a]	Compounds	IC_{50} (μM)
iso-Butyl	**3c**	2.89 ± 0.12	**2c**	0.165 ± 0.014
n-Pentyl	**3e**	3.86 ± 0.15	**2e**	0.174 ± 0.013
n-Hexyl	**3i**	4.59 ± 0.21	**2i**	0.153 ± 0.012
Benzyl	**3k**	2.10 ± 0.18	**2k**	0.094 ± 0.009
Methyl	**3u**	n.a.[b]	/	/

[a] Values are means ± SD of three independent experiments.
[b] n.a.: not active (<60% inhibition at 10 μM).

series of XO inhibitors based on a 1,2,3-triazole-4-carboxylic acid scaffold [42]. In addition, it seemed that the branched alkoxy derivatives usually possessed higher potency than their linear alkoxy counterparts (*e.g.*, **2b** versus **2c**, **2d**). Among this sub-series, compounds **2j** displayed a relatively high potency with an IC_{50} value of 0.092 μM.

In the 4′-benzyloxy derivatives (**2k-t**), compound **2k** (IC_{50} = 0.094 μM) bearing a 4′-benzyloxy group showed considerable potency to compound **2j** (IC_{50} = 0.092 μM). When the benzyl group was substituted by methyl, methoxy or cyano, some derivatives observed further improved potency, such as compounds **2l** (IC_{50} = 0.053 μM), **2m** (IC_{50} = 0.044 μM), **2p** (IC_{50} = 0.050 μM), **2q** (IC_{50} = 0.067 μM) and **2s** (IC_{50} = 0.031 μM). In addition, it seemed that the *meta*-derivative usually possessed higher potency than its *ortho*- and *para*-derivatives (*e.g.*, **2m** versus **2l**, **2n**; **2p** versus **2o**, **2q**; **2s** versus **2r**, **2t**). Especially, *meta*-cyanobenzyloxy derivative **2s** presented the highest potency with an IC_{50} value of 0.031 μM. Interestingly, the most preferred 4′-group was a *meta*-cyanobenzyloxy rather than the *ortho*-cyanobenzyloxy group of compound **1**.

In summary, starting from the *N*-phenylisonicotinamide scaffold of **1**, structural optimization successfully identified a promising XO inhibitor **2s** (IC_{50} = 0.031 μM) and achieved a 10-fold gain in potency. Its potency was very close to the positive control topiroxostat (IC_{50} = 0.021 μM). To investigate the inhibition type of compound **2s** on XO, enzyme kinetics studies were performed. The Lineweaver-Burk plot (Fig. 2) revealed that compound **2s** acted as a mixed-type inhibitor with the same inhibition type as compound **1** [29].

2.3. Molecular docking

To foresee the possible interactions of the optimized compound with XO, molecular modeling simulations of **2s** and **1** in the binding pocket of XO were performed with MOE (Molecular Operating Environment, version 2015.1001, Chemical Computing Group Inc., Canada) software. Since the structure of human XO has not been resolved yet, and bovine XO and human XO exhibit 90% sequence identity [43], we have adopted the crystal structure of bovine XO in complex with topiroxostat (PDB code 1V97) [33] as a receptor in the docking calculations.

Using the default GBVI/WSA dG as a docking function, the **2s** and **1** docking scores were −9.16 kcal/mol and −7.83 kcal/mol, respectively. The scoring order was consistent with its XO binding affinity as well as its inhibition potency. As shown in Fig. 3, the *N*-phenylisonicotinamide scaffolds of **2s** and **1** formed a set of the same interactions with XO active pocket. For instance, the pyridine *para*-N accepted an H-bond from Glu1261, the amide NH formed an H-bond with Glu802 carboxy, the carbonyl group linked to the residues Arg880 and Thr1010 via a water (HOH5497) bridge, and the benzyloxy tail was surrounded by some lipophilic amino acid residues (*e.g.*, Leu648, Phe649 and Phe1013) near the outer region of the pocket. The difference was that, due to the larger size, the tetrazole moiety of compound **2s** can be inserted into and closely occupy the Asn768-sub-pocket, where the N-4 atom accepts an H-bond from the Asn768 residue, as expected. This interaction will immensely benefit the binding affinities as well as enzyme inhibitory potency.

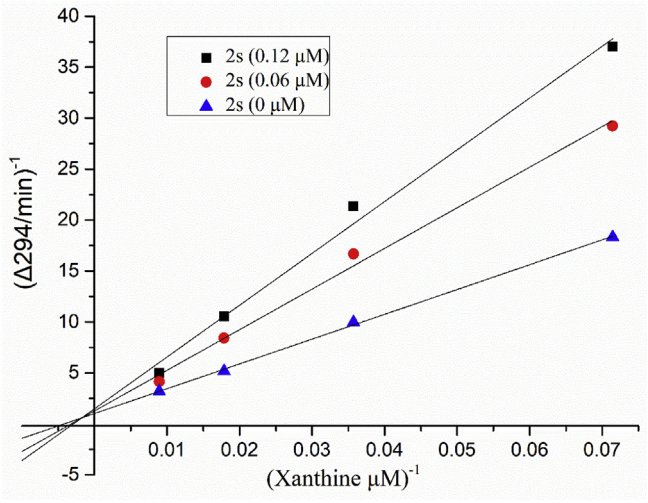

Fig. 2. Lineweaver-Burk plot analysis of XO inhibition by compound **2s.**

2.4. Molecular dynamics (MD) simulations

To obtain a more integrated and precise view of the binding process, a 10 ns MD simulation was performed by starting from the docking pose of compound **2s**. The NAMD software (version 2.13) [44] incorporating in VMD (visual molecular dynamics, version 1.9.3) [45] was adopted for the simulations. The backbone root mean square deviation (RMSD) of the complex calculated by VMD was exhibited in Fig. 3C. It can be seen from Fig. 3C that the RMSD value of the complex tended to be convergent with fluctuations around 2.95 Å after 10 ns of simulation, clearly indicating that the whole system has been equilibrated. The binding model at the end of 10 ns-MD simulation was picked up and rendered with MOE software (Fig. 3B). A set of strong interactions between compound **2s** and XO active pocket were observed as displayed in Fig. 3B. For instance, the N-4 atom of the tetrazole formed a strong H-bond with Asn768, as expected; the pyridine *para*-N and Glu1261 retained the H-bond interaction derived from the docking pose. Although the H-bond between the amide NH and Glu802 residue disappeared, some interesting new interactions emerged on the *m*-cyanobenzyl fragment. After the MD simulation, the *m*-cyanobenzyl tail was folded in the vertical direction of the molecular plane, and as a result, the cyano group was captured by the hydroxyl and amide NH of the Ser876 residue through two H-bonds. Obviously, these interactions may contribute to the ligand-acceptor binding affinity. It also could be an explanation for the excellent potency of compound **2s** compared with its benzyl analogs (*e.g.*, **2k-r** and **2t**).

3. Conclusions

In summary, starting from the *N*-phenylisonicotinamide scaffold

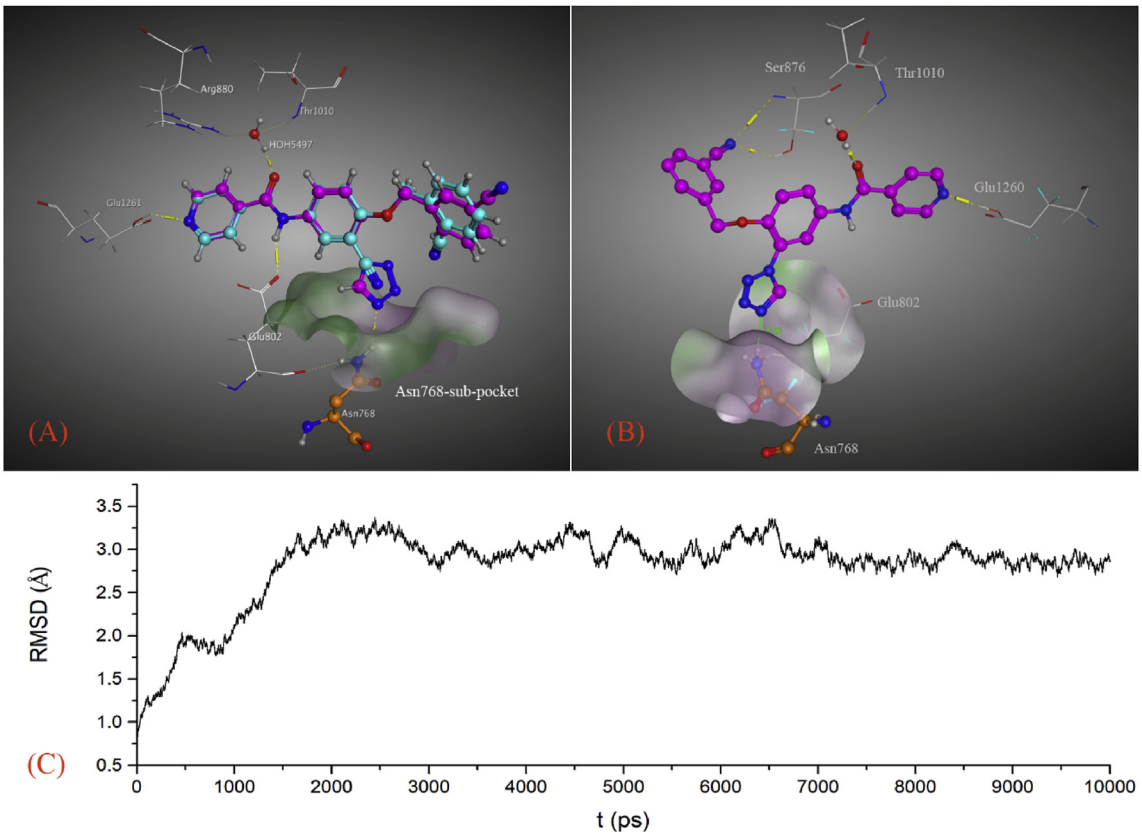

Fig. 3. Results of docking and MD simulations. (A) Docking pose of compound **1** (cyan) and compound **2s** (pink) within the XO binding pocket; (B) MD conformation of compound **2s** (pink) in complex with XO; (C) Backbone RMSD of the complex versus time (10 ns). (For interpretation of the references to colour in this figure legend, the reader is referred to the Web version of this article.)

compound **1**, a series of *N*-(3-(1*H*-tetrazol-1-yl)phenyl)isonicotinamide derivatives was designed and synthesized as novel XO inhibitors by utilizing an SBDD strategy. SAR analysis demonstrated that the 3′-(1*H*-tetrazol-1-yl) moiety greatly improved the inhibitory potency; a 4′-benzyloxy substituent, especially, a 4′-*m*-cyanobenzyloxy, was welcome for the *N*-phenylisonicotinamide scaffold; and the amide-reversal was not beneficial, so maintenance of the *N*-phenylisonicotinamide scaffold was essential. The optimized compound **2s** exhibited a 10-fold gain in potency with an IC_{50} value of 0.031 μM, which was very close to the positive control topiroxostat ($IC_{50} = 0.021$ μM). A Lineweaver-Burk plot showed that compound **2s** acted as a mixed-type XO inhibitor. Molecular docking and MD simulations revealed that the tetrazole moiety could occupy the Asn768-sub-pocket, where the N-4 atom could form an H-bond with the Asn768 residue, as expected. Taken together, compound **2s** has good potential to serve as a new lead compound for the treatment of hyperuricemia and gout, and the further detailed investigation on compound **2s** is under progress.

4. Experimental protocols

4.1. Chemistry

Unless otherwise indicated, reagents and solvents were purchased from commercial sources and used without further purification. All reactions were monitored by TLC using silica gel aluminum cards (0.2 mm thickness) with a fluorescent indicator 254 nm. ^{1}H NMR and ^{13}C NMR spectra were recorded on a Bruker spectrometer. Chemical shifts were expressed in parts per million using tetramethylsilane as an internal reference and DMSO-d_6 as the solvent. ESI-HRMS data were gathered using a Bruker microTOF-Q instrument.

4.1.1. Synthesis of 4-nitro-2-(1H-tetrazol-1-yl)phenol (*4*)

A mixture of 2-amino-4-nitrophenol (10.0 g, 64.9 mmol), triethyl orthoformate (20.7 g, 129.7 mmol) and NaN_3 (8.4 g, 129.7 mmol) in AcOH (100 mL) was heated at 80 °C overnight. The resulted solution was cooled and poured into ice water (200 mL). The formed precipitate was collected by filtration, washed with a large quantity of water and dried to give 4-nitro-2-(1*H*-tetrazol-1-yl)phenol **4** (11.7 g, yield 87.1%) as a brown solid.^{1}H NMR (600 MHz, DMSO-d_6) δ 12.50 (s, 1H), 9.83 (s, 1H), 8.52 (d, $J = 2.8$ Hz, 1H), 8.27 (dd, $J = 9.2$, 2.8 Hz, 1H), 7.28 (d, $J = 9.2$ Hz, 1H).^{13}C NMR (150 MHz, DMSO-d_6) δ 156.92, 144.91, 139.73, 127.22, 122.08, 121.77, 117.82.

4.1.2. Synthesis of 4-amino-2-(1H-tetrazol-1-yl)phenol (*5*)

A mixture of compound **4** (6.0 g, 29.0 mmol), iron powder (6.5 g, 115.8 mmol) and ammonium chloride (3.1 g, 57.9 mmol) in ethanol (90 mL) and water (30 mL) was refluxed overnight. After the completion of the reaction, the mixture was diluted with water (200 mL) and extracted with ethyl acetate (50 mL*3). The oil layer was combined, successively washed with water and brine, dried over anhydrous Na_2SO_4 and evaporated in vacuum to provide 4-amino-2-(1*H*-tetrazol-1-yl)phenol **5** (4.2 g, yield 82.6%) as a yellow solid. ^{1}H NMR (600 MHz, DMSO-d_6) δ 9.71 (s, 1H), 9.59 (s, 1H), 6.90 (d, $J = 2.6$ Hz, 1H), 6.88 (d, $J = 8.7$ Hz, 1H), 6.68 (dd, $J = 8.7$, 2.6 Hz, 1H), 4.92 (s, 2H). ^{13}C NMR (150 MHz, DMSO-d_6) δ 144.68, 142.37, 140.44, 121.92, 118.41, 117.42, 110.04.

*4.1.3. Synthesis of 4-(isonicotinamido)-2-(1H-tetrazol-1-yl)phenyl isonicotinate (**6**)*

Into a solution of 4-amino-2-(1*H*-tetrazol-1-yl)phenol (1.0 g, 5.6 mmol) and triethylamine (5.2 g, 50.8 mmol) in dichloromethane (20 mL) at −5 °C, was added isonicotinoyl chloride (4.0 g, 22.6 mmol) in dichloromethane (20 mL). The mixture was stirred for 1 h at the same temperature. Then, water (80 mL) was added. The oil layer was collected, successively washed with water and brine and evaporated in vacuum to give 4-(isonicotinamido)-2-(1*H*-tetrazol-1-yl)phenyl isonicotinate **6** (1.7 g, 79.4%), as a yellow solid. ^{1}H NMR (600 MHz, DMSO-d_6) δ 10.97 (s, 1H), 10.04 (s, 1H), 8.93−8.80 (m, 4H), 8.38 (d, J = 2.5 Hz, 1H), 8.08 (dd, J = 9.0, 2.5 Hz, 1H), 7.90 (m, 4H), 7.79 (d, J = 9.0 Hz, 1H). ^{13}C NMR (150 MHz, DMSO-d_6) δ 164.92, 163.23, 151.46, 150.87, 144.84, 141.74, 139.13, 138.19, 135.64, 126.53, 125.25, 123.45, 123.35, 122.04, 118.02.

*4.1.4. Synthesis of N-(4-hydroxy-3-(1H-tetrazol-1-yl)phenyl) isonicotinamide (**7**)*

A solution of compound **6** (2.0 g, 5.2 mmol) and sodium hydroxide (1.0 g, 25.8 mmol) in methol (40 mL) and water (15 mL) was heated at 50 °C for 4 h. After the completion of the reaction, the insoluble solid was filtered out and the filtrate was acidized by 5% hydrochloric acid aqueous solution. The formed precipitate was collected by filtration, washed with water and dried to give *N*-(4-hydroxy-3-(1*H*-tetrazol-1-yl)phenyl)isonicotinamide **7** (0.64 g, yield 43.8%) as a yellow solid. ^{1}H NMR (600 MHz, DMSO-d_6) δ 10.72 (s, 1H), 9.82 (s, 1H), 8.75 (d, J = 5.9 Hz, 2H), 8.23 (d, J = 2.5 Hz, 1H), 7.91 (d, J = 6.0 Hz, 2H), 7.80−7.77 (m, 1H), 7.26 (d, J = 8.9 Hz, 1H).^{13}C NMR (150 MHz, DMSO-d_6) δ 164.18, 150.65, 147.24, 144.77, 142.07, 131.11, 123.98, 122.04, 121.26, 117.76, 117.67.

*4.1.5. N-(4-(acetoxy)-3-(1H-tetrazol-1-yl)phenyl)isonicotinamide (**8**)*

A solution of compound **7** (0.2 g, 0.7 mmol) acetyl chloride (0.08 g, 1.1 mmol) and triethylamine (0.14 g, 1.4 mmol) in THF (15 mL) was stirred at room temperature overnight. After the completion of the reaction, the insoluble solid was filtered out. The filtrate was concentrated under reduced pressure and the residue was diluted with water (30 mL). The formed precipitate was collected by filtration, washed by water and dried to give *N*-(4-(acetoxy)-3-(1*H*-tetrazol-1-yl)phenyl)isonicotinamide **7** as a light yellow powder, yield 86.2%. ^{1}H NMR (400 MHz, DMSO-d_6) δ 10.89 (s, 1H), 9.92 (s, 1H), 8.82 (dd, J = 4.5, 1.5 Hz, 2H), 8.30 (d, J = 2.5 Hz, 1H), 8.00 (dd, J = 9.0, 2.5 Hz, 1H), 7.89 (dd, J = 4.4, 1.6 Hz, 2H), 7.59−7.54 (m, 1H), 2.18 (d, J = 5.6 Hz, 3H).^{13}C NMR (100 MHz, DMSO-d_6) δ 168.84, 164.83, 150.88, 144.68, 141.76, 139.36, 137.69, 126.60, 125.26, 123.33, 122.02, 117.78, 40.63, 40.42, 40.21, 40.00, 39.79, 39.58, 39.37, 20.85. ESI-HRMS calcd. for $C_{15}H_{11}N_6O_3$ [M − H]$^-$ 323.0893, found: 323.0892.

*4.1.6. General procedure for the synthesis of N-(4-alkoxy-3-(1H-tetrazol-1-yl)phenyl)isonicotinamides **2a-t***

A mixture of compound **7** (0.71 mmol), alkyl chloride or alkyl bromide (0.85 mmol), anhydrous potassium carbonate (1.4 mmol) and potassium iodide (0.05 mmol) in DMF (10 mL) was stirred under nitrogen atmosphere. When the alkyl chloride or alkyl bromide is a benzyl derivative, the mixture was reacted at 25 °C for 48 h, otherwise, the reaction was heated at 60 °C for 3 h. After that, water (40 mL) was added. The formed precipitate was collected, washed with water and dried to yield a crude product, which was further purified by recrystallization from 50% ethanol to provide corresponding products **2a-t**.

*4.1.6.1. N-(4-isopropoxy-3-(1H-tetrazol-1-yl)phenyl)isonicotinamides (**2a**).* A white powder, yield 87.3%. ^{1}H NMR (600 MHz, DMSO-d_6) δ 10.68 (s, 1H), 9.79 (s, 1H), 8.81 (d, J = 5.4 Hz, 2H), 8.21 (d, J = 2.5 Hz, 1H), 7.93 (dd, J = 9.1, 2.5 Hz, 1H), 7.88 (d, J = 5.9 Hz, 2H), 7.44 (d, J = 9.2 Hz, 1H), 4.79−4.68 (m, 1H), 1.26 (d, J = 6.0 Hz, 6H). ^{13}C NMR (150 MHz, DMSO-d_6) δ 164.27, 150.73, 150.73, 146.49, 144.99, 141.90, 132.41, 123.64, 123.35, 121.89, 121.89, 118.01, 116.13, 72.20, 21.88. ESI-HRMS calcd. for $C_{16}H_{15}N_6O_2$ [M − H]$^-$323.1256, found: 323.1260.

*4.1.6.2. N-(4-butoxy-3-(1H-tetrazol-1-yl)phenyl)isonicotinamides (**2b**).* A light yellow powder, yield 86.5%. ^{1}H NMR (600 MHz, DMSO-d_6) δ 10.68 (s, 1H), 9.79 (s, 1H), 8.81 (d, J = 4.5 Hz, 2H), 8.20 (s, 1H), 7.94 (d, J = 8.5 Hz, 1H), 7.88 (d, J = 4.4 Hz, 2H), 7.42 (d, J = 9.0 Hz, 1H), 4.11 (t, J = 6.1 Hz, 2H), 1.71−1.61 (m, 2H), 1.31 (m, 2H), 0.87 (t, J = 7.3 Hz, 3H). ^{13}C NMR (150 MHz, DMSO-d_6) δ 164.25, 150.72, 150.72, 147.79, 145.01, 141.87, 132.41, 123.72, 122.53, 121.88, 121.88, 118.02, 114.67, 69.19, 30.72, 18.94, 13.96. ESI-HRMS calcd. for $C_{17}H_{17}N_6O_2$ [M − H]$^-$ 337.1413, found: 37.1416.

*4.1.6.3. N-(4-isobutoxy-3-(1H-tetrazol-1-yl)phenyl)isonicotinamides (**2c**).* A white solid, yield 82.4%. ^{1}H NMR (600 MHz, DMSO-d_6) δ 10.69 (s, 1H), 9.79 (s, 1H), 8.81 (d, J = 5.1 Hz, 2H), 8.19 (d, J = 2.5 Hz, 1H), 7.94 (dd, J = 9.0, 2.5 Hz, 1H), 7.89 (dd, J = 4.7, 1.3 Hz, 2H), 7.41 (d, J = 9.1 Hz, 1H), 3.89 (d, J = 6.4 Hz, 2H), 1.98 (m, 1H), 0.87 (d, J = 6.7 Hz, 6H). ^{13}C NMR (150 MHz, DMSO-d_6) δ 164.26, 150.73, 148.08, 145.11, 141.87, 132.40, 123.85, 122.53, 121.88, 118.26, 114.67, 75.45, 27.89, 19.17. ESI-HRMS calcd. for $C_{17}H_{17}N_6O_2$ [M − H]$^-$ 337.1413, found: 337.1416.

*4.1.6.4. N-(4-sec-butoxy-3-(1H-tetrazol-1-yl)phenyl)isonicotinamides (**2d**).* A yellow powder, yield 83.3%. ^{1}H NMR (600 MHz, DMSO-d_6) δ 10.69 (s, 1H), 9.76 (s, 1H), 8.81 (d, J = 5.8 Hz, 2H), 8.21 (d, J = 2.5 Hz, 1H), 7.93 (dd, J = 9.1, 2.5 Hz, 1H), 7.88 (d, J = 5.9 Hz, 2H), 7.43 (d, J = 9.2 Hz, 1H), 4.59−4.46 (m, 1H), 1.64−1.52 (m, 2H), 1.21 (d, J = 6.1 Hz, 3H), 0.81 (t, J = 7.4 Hz, 3H). ^{13}C NMR (150 MHz, DMSO-d_6) δ 164.36, 150.80, 147.03, 145.09, 141.99, 132.48, 123.87, 123.52, 121.96, 118.32, 116.22, 77.00, 28.68, 19.07, 9.57. ESI-HRMS calcd. for $C_{17}H_{17}N_6O_2$ [M − H]$^-$ 337.1413, found: 337.1416.

*4.1.6.5. N-(4-(pentyloxy)-3-(1H-tetrazol-1-yl)phenyl)isonicotinamide (**2e**).* A yellow powder, yield 85.1%.^{1}H NMR (600 MHz, DMSO-d_6) δ 10.68 (s, 1H), 9.80 (s, 1H), 8.81 (d, J = 5.8 Hz, 2H), 8.20 (d, J = 2.4 Hz, 1H), 7.94 (dd, J = 9.0, 2.4 Hz, 1H), 7.89 (d, J = 5.8 Hz, 2H), 7.41 (d, J = 9.1 Hz, 1H), 4.11 (t, J = 6.4 Hz, 2H), 1.68 (m, 2H), 1.27 (dd, J = 8.7, 5.5 Hz, 4H), 0.85 (t, J = 6.8 Hz, 3H). ^{13}C NMR (150 MHz, DMSO-d_6) δ 164.25, 150.72, 147.78, 145.01, 141.88, 132.43, 123.72, 122.55, 121.88, 118.02, 114.70, 69.47, 28.29, 27.82, 22.08, 14.20. ESI-HRMS calcd. for $C_{18}H_{19}N_6O_2$ [M − H]$^-$ 351.1569, found: 351.1572.

*4.1.6.6. N-(4-(isopentyloxy)-3-(1H-tetrazol-1-yl)phenyl)isonicotinamide (**2f**).* A light yellow powder, yield 90.8%. ^{1}H NMR (600 MHz, DMSO-d_6) δ 10.68 (s, 1H), 9.79 (s, 1H), 8.81 (d, J = 4.2 Hz, 2H), 8.21 (d, J = 2.4 Hz, 1H), 7.94 (dd, J = 9.0, 2.3 Hz, 1H), 7.89 (d, J = 5.6 Hz, 2H), 7.43 (d, J = 9.1 Hz, 1H), 4.14 (t, J = 6.3 Hz, 2H), 1.65−1.55 (m, 3H), 0.86 (d, J = 6.3 Hz, 6H). ^{13}C NMR (150 MHz, DMSO-d_6) δ 164.24, 150.72, 147.78, 144.99, 141.86, 132.42, 123.71, 122.52, 121.88, 118.02, 114.65, 68.03, 37.37, 24.96, 22.69. ESI-HRMS calcd. for $C_{18}H_{19}N_6O_2$ [M − H]$^-$ 351.1569, found: 351.1572.

*4.1.6.7. N-(4-(cyclopentyloxy)-3-(1H-tetrazol-1-yl)phenyl)isonicotinamide (**2g**).* A white powder, yield 78.3%.^{1}H NMR (600 MHz, DMSO-d_6) δ 10.69 (s, 1H), 9.75 (s, 1H), 8.81 (d, J = 5.7 Hz, 2H), 8.21 (d, J = 2.4 Hz, 1H), 7.93 (dd, J = 9.0, 2.5 Hz, 1H), 7.88 (d, J = 5.8 Hz, 2H), 7.41 (d, J = 9.1 Hz, 1H), 5.04−4.84 (m, 1H), 1.87 (m, 2H), 1.73−1.63 (m, 2H), 1.54 (t, J = 7.1 Hz, 4H). ^{13}C NMR (150 MHz, DMSO-d_6) δ 164.36, 150.80, 146.80, 144.99, 142.00, 132.45, 123.76,

123.40, 121.96, 118.20, 116.04, 81.43, 32.53, 23.76. ESI-HRMS calcd. for $C_{18}H_{17}N_6O_2$ $[M-H]^-$ 349.1413, found: 349.1416.

*4.1.6.8. N-(4-((2-ethylpropanyl)oxy)-3-(1H-tetrazol-1-yl)phenyl)isonicotinamide (**2h**).* An off-white powder, yield 78.3%. ^{1}H NMR (500 MHz, DMSO-d_6) δ 10.76 (s, 1H), 9.74 (d, J = 9.8 Hz, 1H), 8.80 (d, J = 4.8 Hz, 2H), 8.21 (s, 1H), 7.94 (d, J = 9.1 Hz, 1H), 7.90 (d, J = 4.8 Hz, 2H), 7.43 (d, J = 9.1 Hz, 1H), 4.43–4.35 (m, 1H), 1.61–1.50 (m, 4H), 0.78 (t, J = 7.4 Hz, 6H).^{13}C NMR (125 MHz, DMSO-d_6) δ 163.71, 150.16, 146.92, 144.52, 141.32, 131.79, 123.35, 122.78, 121.37, 117.84, 115.49, 81.04, 24.90, 8.79. ESI-HRMS calcd. for $C_{18}H_{19}N_6O_2$ $[M-H]^-$ 351.1569, found: 351.1573.

*4.1.6.9. N-(4-(hexyloxy)-3-(1H-tetrazol-1-yl)phenyl)isonicotinamide (**2i**).* A light yellow powder, yield 80.2%. ^{1}H NMR (600 MHz, DMSO-d_6) δ 10.68 (s, 1H), 9.80 (s, 1H), 8.81 (d, J = 5.8 Hz, 2H), 8.20 (d, J = 2.4 Hz, 1H), 7.94 (dd, J = 9.0, 2.4 Hz, 1H), 7.89 (d, J = 5.9 Hz, 2H), 7.41 (d, J = 9.1 Hz, 1H), 4.11 (t, J = 6.4 Hz, 2H), 1.70–1.63 (m, 2H), 1.29–1.20 (m, 6H), 0.84 (t, J = 6.8 Hz, 3H). ^{13}C NMR (150 MHz, DMSO-d_6) δ 164.25, 150.72, 147.78, 145.01, 141.87, 132.42, 123.72, 122.55, 121.88, 118.02, 114.70, 69.48, 31.16, 28.57, 25.29, 22.34, 14.18. ESI-HRMS calcd. for $C_{19}H_{21}N_6O_2$ $[M-H]^-$ 365.1726, found: 365.1728.

*4.1.6.10. N-(4-(octyloxy)-3-(1H-tetrazol-1-yl)phenyl)isonicotinamide (**2j**).* A white powder, yield 77.3%. ^{1}H NMR (600 MHz, DMSO-d_6) δ 10.68 (s, 1H), 9.79 (s, 1H), 8.81 (dd, J = 4.5, 1.5 Hz, 2H), 8.21 (d, J = 2.5 Hz, 1H), 7.94 (dd, J = 9.1, 2.5 Hz, 1H), 7.89 (dd, J = 4.5, 1.5 Hz, 2H), 7.41 (d, J = 9.1 Hz, 1H), 4.10 (t, J = 6.4 Hz, 2H), 1.70–1.64 (m, 2H), 1.28–1.19 (m, 10H), 0.86 (t, J = 7.1 Hz, 3H). ^{13}C NMR (150 MHz, DMSO-d_6) δ 164.23, 150.72, 147.73, 144.97, 141.86, 132.43, 123.67, 122.55, 121.87, 117.96, 114.68, 69.48, 31.52, 28.94, 28.61, 25.64, 22.44, 14.31. ESI-HRMS calcd. for $C_{21}H_{25}N_6O_2$ $[M-H]^-$ 393.2039, found: 393.2041.

*4.1.6.11. N-(4-(benzyloxy)-3-(1H-tetrazol-1-yl)phenyl)isonicotinamide (**2k**).* A yellow powder, yield 88.6%. ^{1}H NMR (600 MHz, DMSO-d_6) δ 10.72 (s, 1H), 9.85 (s, 1H), 8.81 (d, J = 4.9 Hz, 2H), 8.23 (d, J = 2.5 Hz, 1H), 7.95 (dd, J = 9.1, 2.5 Hz, 1H), 7.89 (d, J = 5.9 Hz, 2H), 7.51 (d, J = 9.1 Hz, 1H), 7.39 (s, 2H), 7.38 (d, J = 1.5 Hz, 2H), 7.36–7.31 (m, 1H), 5.27 (s, 2H). ^{13}C NMR (150 MHz, DMSO-d_6) δ 164.41, 150.82, 147.58, 145.13, 141.96, 136.53, 132.88, 128.98, 128.59, 128.02, 123.81, 122.97, 121.96, 118.35, 115.44, 71.14. ESI-HRMS calcd. for $C_{20}H_{15}N_6O_2$ $[M-H]^-$ 372.1256, found: 371.1259.

*4.1.6.12. N-(4-((2-methylbenzyl)oxy)-3-(1H-tetrazol-1-yl)phenyl)isonicotinamide(**2l**).* A yellow powder, yield 78.3%. ^{1}H NMR (600 MHz, DMSO-d_6) δ 10.74 (s, 1H), 9.77 (s, 1H), 8.81 (d, J = 5.7 Hz, 2H), 8.20 (d, J = 2.5 Hz, 1H), 7.97 (dd, J = 9.1, 2.5 Hz, 1H), 7.90 (d, J = 5.9 Hz, 2H), 7.58 (d, J = 9.1 Hz, 1H), 7.30 (d, J = 7.4 Hz, 1H), 7.24 (t, J = 7.0 Hz, 1H), 7.18 (m, 2H), 5.25 (s, 2H), 2.20 (s, 3H). ^{13}C NMR (150 MHz, DMSO-d_6) δ 164.40, 150.81, 147.91, 145.16, 141.95, 136.91, 134.40, 132.86, 130.67, 128.78, 128.76, 126.27, 123.99, 122.95, 121.97, 118.65, 115.54, 69.83, 18.71. ESI-HRMS calcd. for $C_{21}H_{17}N_6O_2$ $[M-H]^-$ 385.1413, found: 385.1416.

*4.1.6.13. N-(4-((3-methylbenzyl)oxy)-3-(1H-tetrazol-1-yl)phenyl)isonicotinamide (**2m**).* A yellow powder, yield 76.9%. ^{1}H NMR (600 MHz, DMSO-d_6) δ 10.72 (s, 1H), 9.85 (s, 1H), 8.81 (dd, J = 4.5, 1.4 Hz, 2H), 8.23 (d, J = 2.5 Hz, 1H), 7.95 (dd, J = 9.1, 2.6 Hz, 1H), 7.89 (dd, J = 4.5, 1.5 Hz, 2H), 7.50 (d, J = 9.1 Hz, 1H), 7.26 (t, J = 7.8 Hz, 1H), 7.17 (d, J = 7.2 Hz, 2H), 7.14 (d, J = 7.5 Hz, 1H), 5.22 (s, 2H), 2.30 (s, 3H). ^{13}C NMR (150 MHz, DMSO-d_6) δ 164.40, 150.81, 147.60, 145.13, 141.96, 138.16, 136.45, 132.89, 129.19, 128.88, 128.57, 125.07, 123.81, 123.01, 121.97, 118.31, 115.49, 71.24, 21.41. ESI-HRMS calcd. for $C_{21}H_{17}N_6O_2$ $[M-H]^-$ 385.1413, found: 385.1416.

*4.1.6.14. N-(4-((4-methylbenzyl)oxy)-3-(1H-tetrazol-1-yl)phenyl)isonicotinamide (**2n**).* A yellow powder, yield 80.5%. ^{1}H NMR (600 MHz, DMSO-d_6) δ 10.69 (s, 1H), 9.81 (s, 1H), 8.81 (d, J = 5.6 Hz, 2H), 8.21 (d, J = 2.4 Hz, 1H), 7.93 (dd, J = 9.1, 2.5 Hz, 1H), 7.88 (d, J = 5.9 Hz, 2H), 7.50 (d, J = 9.1 Hz, 1H), 7.27 (d, J = 7.9 Hz, 2H), 7.18 (d, J = 7.8 Hz, 2H), 5.20 (s, 2H), 2.29 (s, 3H). ^{13}C NMR (150 MHz, DMSO-d_6) δ 164.29, 150.73, 147.43, 145.02, 141.86, 137.86, 133.34, 132.70, 129.45, 128.15, 123.64, 122.81, 121.88, 118.13, 115.31, 70.95, 21.14. ESI-HRMS calcd. for $C_{21}H_{17}N_6O_2$ $[M-H]^-$ 385.1413, found: 385.1416.

*4.1.6.15. N-(4-((2-methoxybenzyl)oxy)-3-(1H-tetrazol-1-yl)phenyl)isonicotinamide (**2o**).* A yellow powder, yield 79.3%. ^{1}H NMR (600 MHz, DMSO-d_6) δ 10.72 (s, 1H), 9.73 (s, 1H), 8.82 (d, J = 4.1 Hz, 2H), 8.24 (d, J = 2.5 Hz, 1H), 7.96 (dd, J = 9.1, 2.5 Hz, 1H), 7.90 (d, J = 5.8 Hz, 2H), 7.53 (d, J = 9.1 Hz, 1H), 7.37–7.32 (m, 1H), 7.30 (d, J = 7.4 Hz, 1H), 7.05 (d, J = 8.2 Hz, 1H), 6.94 (t, J = 7.4 Hz, 1H), 5.23 (s, 2H), 3.80 (s, 3H). ^{13}C NMR (150 MHz, DMSO-d_6) δ 164.28, 157.36, 150.68, 147.34, 144.86, 141.89, 132.85, 130.24, 129.63, 123.91, 123.60, 123.02, 121.93, 120.68, 117.87, 115.66, 111.36, 67.04, 55.76. ESI-HRMS calcd. for $C_{21}H_{17}N_6O_3$ $[M-H]^-$ 401.1362, found: 401.1365.

*4.1.6.16. N-(4-((3-methoxy-cyanobenzyl)oxy)-3-(1H-tetrazol-1-yl)phenyl)isonicotinamide (**2p**).* An off-white powder, yield 67.3%. ^{1}H NMR (500 MHz, DMSO-d_6) δ 10.73 (s, 1H), 9.87 (s, 1H), 8.80 (s, 2H), 8.22 (s, 1H), 7.94 (d, J = 8.9 Hz, 1H), 7.88 (s, 2H), 7.48 (d, J = 8.8 Hz, 1H), 7.28 (t, J = 7.3 Hz, 1H), 6.93 (s, 2H), 6.88 (d, J = 8.0 Hz, 1H), 5.22 (s, 2H), 3.74 (s, 3H). ^{13}C NMR (125 MHz, DMSO-d_6) δ 163.77, 159.21, 150.16, 146.90, 144.56, 141.41, 137.47, 132.42, 129.44, 123.23, 122.32, 121.34, 119.33, 117.76, 114.74, 113.54, 112.61, 70.29, 54.85. ESI-HRMS calcd. for $C_{21}H_{17}N_6O_3$ $[M-H]^-$ 401.1362, found: 401.1365.

*4.1.6.17. N-(4-((4-methoxy-cyanobenzyl)oxy)-3-(1H-tetrazol-1-yl)phenyl)isonicotinamide (**2q**).* An off-white powder, yield 65.9%. ^{1}H NMR (600 MHz, DMSO-d_6) δ 10.67 (s, 1H), 9.77 (s, 1H), 8.81 (d, J = 4.8 Hz, 2H), 8.21 (d, J = 2.4 Hz, 1H), 7.94 (dd, J = 9.0, 2.4 Hz, 1H), 7.88 (d, J = 5.8 Hz, 2H), 7.51 (d, J = 9.1 Hz, 1H), 7.33 (d, J = 8.5 Hz, 2H), 6.93 (d, J = 8.6 Hz, 2H), 5.17 (s, 2H), 3.75 (s, 3H). ^{13}C NMR (150 MHz, DMSO-d_6) δ 164.39, 159.69, 150.82, 147.55, 145.04, 141.97, 132.80, 129.97, 128.32, 123.73, 122.99, 121.96, 118.19, 115.55, 114.39, 71.01, 55.57. ESI-HRMS calcd. for $C_{21}H_{17}N_6O_3$ $[M-H]^-$ 401.1362, found: 401.1365.

*4.1.6.18. N-(4-((2-cyanobenzyl)oxy)-3-(1H-tetrazol-1-yl)phenyl)isonicotinamide (**2r**).* An off-white powder, yield 72.3%. ^{1}H NMR (500 MHz, DMSO-d_6) δ 10.77 (s, 1H), 9.75 (s, 1H), 8.80 (d, J = 3.5 Hz, 2H), 8.23 (s, 1H), 7.97 (d, J = 9.0 Hz, 1H), 7.88 (s, 3H), 7.74 (t, J = 7.3 Hz, 1H), 7.64 (d, J = 7.6 Hz, 1H), 7.59–7.54 (m, 2H), 5.43 (s, 2H). ^{13}C NMR (125 MHz, DMSO-d_6) δ 163.83, 150.18, 146.43, 144.36, 141.34, 138.90, 133.32, 133.18, 132.82, 129.17, 129.13, 123.17, 122.43, 121.35, 117.77, 116.85, 114.90, 110.81, 68.76. ESI-HRMS calcd. for $C_{21}H_{14}N_7O_2$ $[M-H]^-$ 396.1209, found: 396.1212.

*4.1.6.19. N-(4-((3-cyanobenzyl)oxy)-3-(1H-tetrazol-1-yl)phenyl)isonicotinamide (**2s**).* An off-white powder, yield 81.2%. ^{1}H NMR (600 MHz, DMSO-d_6) δ 10.72 (s, 1H), 9.91 (s, 1H), 8.82 (d, J = 5.6 Hz, 2H), 8.24 (d, J = 2.3 Hz, 1H), 7.96 (dd, J = 9.0, 2.3 Hz, 1H), 7.89 (d, J = 5.7 Hz, 3H), 7.82 (d, J = 7.7 Hz, 1H), 7.74 (d, J = 7.8 Hz, 1H), 7.61 (t, J = 7.7 Hz, 1H), 7.49 (d, J = 9.1 Hz, 1H), 5.33 (s, 2H). ^{13}C NMR (150 MHz, DMSO-d_6) δ 164.42, 150.82, 147.16, 145.22, 141.92, 138.24, 133.12, 132.78, 132.40, 131.53, 130.26, 123.78, 122.96, 121.97, 119.05, 118.39, 115.33, 112.02, 69.95. ESI-HRMS calcd. for $C_{21}H_{14}N_7O_2$ $[M-H]^-$ 396.1209, found: 396.1212.

*4.1.6.20. N-(4-((4-cyanobenzyl)oxy)-3-(1H-tetrazol-1-yl)phenyl)isonicotinamide (**2t**).* A yellow powder, yield 65.6%. ^{1}H NMR (500 MHz, DMSO-d_6) δ 10.74 (s, 1H), 9.90 (s, 1H), 8.80 (s, 2H), 8.22 (s, 1H), 7.91 (d, J = 34.5 Hz, 5H), 7.57 (s, 2H), 7.46 (s, 1H), 5.37 (s, 2H).^{13}C NMR (125 MHz, DMSO-d_6) δ 163.79, 150.17, 146.56, 144.55, 141.61, 141.33, 132.56, 132.31, 127.84, 123.19, 122.30, 121.33, 118.46, 117.86, 114.65, 110.65, 69.49. ESI-HRMS calcd. for $C_{21}H_{14}N_7O_2$ [M − H]$^-$ 396.1209, found: 396.1212.

*4.1.7. Synthesis of 4-hydroxy-3-(1H-tetrazol-1-yl)benzoic acid (**9**)*

A mixture of 3-amino-4-hydroxybenzoic acid (5.0 g, 33 mmol), triethyl orthoformate (14.5 g, 98 mmol) and NaN_3 (4.3 g, 65 mmol) in AcOH (50 mL) was reacted at 80 °C overnight. Then, 15% hydrochloric acid aqueous solution (50 mL) was added. After stirring at 80 °C for 1 h, the mixture was cooled and allowed to stand for 3 h. The formed precipitate was filtered, washed with water and dried to yield 4-hydroxy-3-(1*H*-tetrazol-1-yl)benzoic acid (4.5 g, 67.0%) as an off-white solid. ^{1}H NMR (400 MHz, DMSO-d_6) δ 12.89 (s, 1H), 11.78 (s, 1H), 9.82 (s, 1H), 8.16 (d, J = 2.1 Hz, 1H), 8.00 (dd, J = 8.6, 2.1 Hz, 1H), 7.22 (d, J = 8.6 Hz, 1H). ^{13}C NMR (100 MHz, DMSO-d_6) δ 166.58, 154.70, 144.97, 132.95, 127.40, 122.68, 121.76, 117.45.

*4.1.8. General procedure for the synthesis of 4-alkoxy-3-(1H-tetrazol-1-yl)benzoic acid (**11**)*

A mixture of compound **9** (4.9 mmol), alkyl chloride or alkyl bromide (12.1 mmol), anhydrous potassium carbonate (24.3 mmol) and potassium iodide (0.5 mmol) in DMF (15 mL) was stirred at 60 °C for 6 h. The insoluble solid was filtered off and the filtrate was diluted with water (50 mL). The formed precipitate was collected by filtration, washed with a large quantity of water and dried to give the corresponding intermediates alkyl 4-alkoxy-3-(1*H*-tetrazol-1-yl)benzoates **10**, which was directly used in the next step without further purification.

A solution of prepared compound **10** and sodium hydroxide (9.8 mmol) in methanol (20 mL) and water (20 mL) was heated at 50 °C for 30 min. After the completion of the reaction, the solution was cooled to −5 °C, acidized to pH 3–4 with 5% hydrochloric acid aqueous solution and allowed to stand for 5 h. The formed precipitate was collected by filtration, washed with water and dried to give the corresponding key intermediates 4-alkoxy-3-(1*H*-tetrazol-1-yl)benzoic acids (**11c**, **11e**, **11i**, **11k** and **11u**).

*4.1.8.1. 4-Isobutoxy-3-(1H-tetrazol-1-yl)benzoic acid (**11c**).* A yellow powder, yield 68.8%. ^{1}H NMR (600 MHz, DMSO-d_6) δ 13.12 (s, 1H), 9.76 (s, 1H), 8.17 (d, J = 2.0 Hz, 1H), 8.13 (dd, J = 8.7, 2.1 Hz, 1H), 7.44 (d, J = 8.8 Hz, 1H), 3.95 (d, J = 6.4 Hz, 2H), 1.97 (m, 1H), 0.85 (d, J = 6.7 Hz, 6H). ^{13}C NMR (150 MHz, DMSO-d_6) δ 166.39, 155.46, 145.24, 133.50, 127.65, 123.92, 122.96, 114.16, 75.67, 27.87, 19.12.

*4.1.8.2. 4-(pentyloxy)-3-(1H-tetrazol-1-yl)benzoic acid (**11e**).* A yellow powder, yield 76.8%. ^{1}H NMR (600 MHz, DMSO-d_6) δ 13.08 (s, 1H), 9.76 (s, 1H), 8.17 (d, J = 2.1 Hz, 1H), 8.12 (dd, J = 8.7, 2.1 Hz, 1H), 7.45 (d, J = 8.8 Hz, 1H), 4.17 (t, J = 6.5 Hz, 2H), 1.68 (p, J = 6.8 Hz, 2H), 1.28–1.24 (m, 4H), 0.83 (m, 3H). ^{13}C NMR (150 MHz, DMSO-d_6) δ 166.38, 155.19, 145.13, 133.36, 127.40, 123.92, 122.98, 114.22, 69.89, 28.19, 27.81, 22.11, 14.22.

*4.1.8.3. 4-(hexyloxy)-3-(1H-tetrazol-1-yl)benzoic acid (**11i**).* A yellow powder, yield 64.2%. ^{1}H NMR (600 MHz, DMSO-d_6) δ 13.03 (s, 1H), 9.76 (s, 1H), 8.16 (d, J = 2.1 Hz, 1H), 8.12 (dd, J = 8.7, 2.1 Hz, 1H), 4.17 (t, J = 6.4 Hz, 2H), 1.70–1.63 (m, 2H), 1.28–1.20 (m, 6H), 0.82 (t, J = 6.9 Hz, 3H).^{13}C NMR (150 MHz, DMSO-d_6) δ 166.35, 155.18, 145.13, 133.35, 127.38, 123.95, 122.98, 114.22, 69.90, 31.19, 28.47, 25.27, 22.38, 14.20.

*4.1.8.4. 4-(benzyloxy)-3-(1H-tetrazol-1-yl)benzoic acid (**11k**).* An off-white powder, yield 78.8%. ^{1}H NMR (600 MHz, DMSO-d_6) δ 13.07 (s, 1H), 9.81 (s, 1H), 8.22 (d, J = 2.1 Hz, 1H), 8.15 (dd, J = 8.7, 2.1 Hz, 1H), 7.54 (d, J = 8.8 Hz, 1H), 7.38 (q, J = 7.9 Hz, 4H), 7.33 (m, 2H), 5.33 (d, J = 4.9 Hz, 2H).^{13}C NMR (150 MHz, DMSO-d_6) δ 166.38, 154.83, 145.18, 136.02, 133.33, 129.01, 128.70, 128.01, 127.61, 124.47, 123.20, 114.73, 71.27.

*4.1.8.5. 4-Methoxy-3-(1H-tetrazol-1-yl)benzoic acid (**11u**).* An off-white powder, yield 58.7%. ^{1}H NMR (400 MHz, DMSO-d_6) δ 13.15 (s, 1H), 9.84 (s, 1H), 8.18 (d, J = 2.1 Hz, 1H), 8.15 (dd, J = 8.7, 2.1 Hz, 1H), 7.47 (d, J = 8.8 Hz, 1H), 3.95 (s, 3H). ^{13}C NMR (100 MHz, DMSO-d_6) δ 166.38, 155.70, 145.22, 133.38, 127.32, 124.08, 122.86, 113.63, 57.36.

*4.1.9. General procedure for the synthesis of 4-alkoxy-N-(pyridin-4-yl)-3-(1H-tetrazol-1-yl)benzamides **3***

A solution of compound **11** (4.0 mmol) in thionyl chloride (10 mL) containing two drops of DMF was heated at 50 °C for 5 h. After that, The extra thionyl chloride was evaporated in vacuum and the precipitate was added THF (20 mL) to yield a suspension of 4-alkoxy-3-(1*H*-tetrazol-1-yl)benzoyl chloride hydrochloride **12**.

The freshly prepared compound **12** suspensions were slowly dropwise added into a solution of pyridin-4-amine (6.0 mmol) and triethylamine (12.0 mmol) in THF (30 mL) at −10 °C. The mixture was maintained at the same temperature for 1 h and then stirred at room temperature overnight. The insoluble materials were removed by filtration and washed with THF. The filtrate was evaporated in vacuum to remove about 2/3 of the solvent. The residue was dispersed into water, filtered under reduced pressure, washed and dried to provide crude products, which was further purified by recrystallization from 50% ethanol to provide corresponding 4-alkoxy-*N*-(pyridin-4-yl)-3-(1*H*-tetrazol-1-yl)benzamides **3c**, **3e**, **3i**, **3k** and **3u**.

*4.1.9.1. 4-Isobutoxy-N-(pyridin-4-yl)-3-(1H-tetrazol-1-yl)benzamide (**3c**).* A yellow powder, yield 62.2%. ^{1}H NMR (400 MHz, DMSO-d_6) δ 10.59 (s, 1H), 9.82 (s, 1H), 8.48 (d, J = 5.7 Hz, 2H), 8.35 (d, J = 2.2 Hz, 1H), 8.25 (dd, J = 8.8, 2.2 Hz, 1H), 7.78 (d, J = 6.3 Hz, 2H), 7.52 (d, J = 8.9 Hz, 1H), 3.98 (d, J = 6.4 Hz, 2H), 1.98 (m, 1H), 0.87 (d, J = 6.7 Hz, 6H). ^{13}C NMR (100 MHz, DMSO-d_6) δ 164.78, 155.03, 150.78, 146.28, 145.40, 132.37, 126.80, 126.51, 122.80, 114.53, 114.15, 75.69, 27.92, 19.16. ESI-HRMS calcd. for $C_{17}H_{17}N_6O_2$ [M − H]$^-$ 337.1413, found: 337.1417.

*4.1.9.2. 4-(pentyloxy)-N-(pyridin-4-yl)-3-(1H-tetrazol-1-yl)benzamide (**3e**).* A yellow powder, yield 73.1%. ^{1}H NMR (400 MHz, DMSO-d_6) δ 10.59 (s, 1H), 9.82 (s, 1H), 8.48 (d, J = 6.0 Hz, 2H), 8.36 (d, J = 2.2 Hz, 1H), 8.24 (dd, J = 8.8, 2.3 Hz, 1H), 7.78 (dd, J = 4.9, 1.4 Hz, 2H), 7.52 (d, J = 8.9 Hz, 1H), 4.19 (t, J = 6.5 Hz, 2H), 1.69 (p, J = 6.8 Hz, 2H), 1.27 (m, 4H), 0.83 (t, J = 7.1 Hz, 3H). ^{13}C NMR (100 MHz, DMSO-d_6) δ 164.79, 154.71, 150.77, 146.28, 145.28, 132.23, 126.82, 126.24, 122.80, 114.53, 114.16, 69.89, 28.22, 27.83, 22.14, 14.26. ESI-HRMS calcd. for $C_{18}H_{19}N_6O_2$ [M − H]$^-$ 351.1569, found: 351.1573.

*4.1.9.3. 4-(hexyloxy)-N-(pyridin-4-yl)-3-(1H-tetrazol-1-yl)benzamide (**3i**).* A yellow powder, yield 81.2%. ^{1}H NMR (600 MHz, DMSO-d_6) δ 10.62 (s, 1H), 9.84 (s, 1H), 8.49 (t, J = 8.6 Hz, 2H), 8.37 (d, J = 2.2 Hz, 1H), 8.25 (dd, J = 8.8, 2.2 Hz, 1H), 7.80 (dd, J = 5.0, 1.4 Hz, 2H), 7.54 (d, J = 8.9 Hz, 1H), 4.21 (t, J = 6.4 Hz, 2H), 1.72–1.67 (m, 2H), 1.31–1.22 (m, 6H), 0.84 (t, J = 6.8 Hz, 3H). ^{13}C NMR (150 MHz, DMSO-d_6) δ 164.80, 154.71, 150.78, 146.29, 145.32, 132.24, 126.79, 126.25, 122.78, 114.52, 114.15, 69.89, 31.22, 28.49, 25.31, 22.43, 14.26. ESI-HRMS calcd. for $C_{19}H_{21}N_6O_2$ [M − H]$^-$ 365.1726, found: 365.1729.

*4.1.9.4. 4-(benzyloxy)-N-(pyridin-4-yl)-3-(1H-tetrazol-1-yl)benzamide (**3k**).* A yellow powder, yield 72.8%. ^{1}H NMR (600 MHz, DMSO-d_6) δ 10.63 (s, 1H), 9.89 (s, 1H), 8.48 (t, J = 8.2 Hz, 2H), 8.38 (d, J = 2.2 Hz, 1H), 8.25 (dd, J = 8.8, 2.2 Hz, 1H), 7.78 (dd, J = 5.0, 1.3 Hz, 2H), 7.63−7.61 (m, 1H), 7.41−7.37 (m, 4H), 7.35−7.32 (m, 1H), 5.37 (s, 2H). ^{13}C NMR (150 MHz, DMSO-d_6) δ 164.82, 154.34, 150.81, 146.27, 145.39, 136.06, 132.20, 129.05, 128.72, 128.03, 127.27, 126.51, 123.01, 114.70, 114.52, 71.19. ESI-HRMS calcd. for $C_{20}H_{15}N_6O_2$ $[M-H]^-$ 371.1256, found: 371.1261.

*4.1.9.5. 4-Methoxy-N-(pyridin-4-yl)-3-(1H-tetrazol-1-yl)benzamide (**3u**).* An off-white powder, yield 77.8%. ^{1}H NMR (600 MHz, DMSO-d_6) δ 10.65 (s, 1H), 9.90 (s, 1H), 8.49 (dd, J = 4.9, 1.4 Hz, 2H), 8.37 (d, J = 2.3 Hz, 1H), 8.28 (dd, J = 8.8, 2.3 Hz, 1H), 7.79 (dd, J = 4.8, 1.5 Hz, 2H), 7.56 (d, J = 8.9 Hz, 1H), 3.98 (s, 3H).^{13}C NMR (150 MHz, DMSO-d_6) δ 164.84, 155.26, 150.77, 146.31, 145.39, 132.28, 126.98, 126.22, 122.66, 114.54, 113.56, 57.41. ESI-HRMS calcd. for $C_{14}H_{11}N_6O_2$ $[M-H]^-$ 295.0943, found: 295.0950.

4.2. Assay of in vitro XO inhibitory activity

Bovine XO inhibitory potency in vitro was assayed spectrophotometrically by measuring the uric acid formation at 294 nm at 25 °C. The testing method was based on the procedure reported by Matsumoto et al. [30], with modification. The assay mixture contained 0.1 M sodium pyrophosphate buffer (pH 8.3), 0.3 mM Na_2EDTA, 1 mM xanthine, 25 U/L XO (Sigma, X1875), and the test compound. The enzyme was pre-incubated for 10 min with the test compound, and the reaction was started by the addition of xanthine. The XO inhibition by various compounds was calculated by the reduction of uric acid production in the first 2 min. All tests were performed in triplicate. Compounds presenting inhibitory effects over 60% at a concentration of 10 μM were further tested at a wide range of concentrations to calculate their IC_{50} values using SPSS 20.0 software.

4.3. Molecular docking

Molecular modeling studies were carried out with MOE (Molecular Operating Environment, version 2015.1001) software by a similar procedure reported in our previous studies [29]. The crystal structure of bovine XO in complex with topiroxostat (PDB code 1V97) [33] downloaded from RCSB Protein Data Bank was adopted in docking calculations. The receptor was optimized by a Quickprep protocol with the following procedures of Structure Preparation, Protonate 3D and Structure Refine (RMSD gradient = 0.1 kcal/mol, AMBER10: EHT field) [46]. The docking procedure was adopted the standard protocol implemented in MOE and all parameters were maintained as the defaults.

4.4. MD simulations

MD simulations were performed with NAMD software (version 2.13) [44] incorporating in VMD (visual molecular dynamics, version 1.9.3) [45]. The protein was described by using CHARMM22 force field. Ligand parameterization was carried out using CHARMM General Force Field (CGenFF) server (https://cgenff.umaryland.edu/) which performed ligand atom typing and assignment of parameters and charges by analogy [47]. All the systems were solvated using the TIP3 water model and neutralized by the addition of NaCl. Minimization for 1000 steps was carried out by the steepest descent method and the system equilibrated for 1 ns in NVT ensemble. Unrestrained 10 ns-production-MD simulations was performed at constant temperature (300 K) and pressure (1 atm) in (NPT) ensemble at a time step of 2 fs. The results were analyzed in VMD and the binding model at the end of 10 ns-MD simulation was rendered in MOE software.

Acknowledgments

This work was supported by the National Natural Science Foundation of China (Grant Nos. 81803355 and 81573687), the Scientific Research Fund of Liaoning Provincial Education Department (LQNK201739) and the Doctoral Research Funding (229181).

Appendix A. Supplementary data

Supplementary data to this article can be found online at https://doi.org/10.1016/j.ejmech.2019.111717.

References

[1] G. Luna, A.V. Dolzhenko, R.L. Mancera, Inhibitors of xanthine oxidase: scaffold diversity and structure-based drug design, ChemMedChem 14 (2019) 714−743.
[2] Z. Smelcerovic, A. Veljkovic, G. Kocic, D. Yancheva, Z. Petronijevic, M. Anderluh, A. Smelcerovic, Xanthine oxidase inhibitory properties and anti-inflammatory activity of 2-amino-5-alkylidene-thiazol-4-ones, Chem. Biol. Interact. 229 (2015) 73−81.
[3] A. Šmelcerović, K. Tomović, Ž. Šmelcerović, Ž. Petronijević, G. Kocić, T. Tomašič, Ž. Jakopin, M. Anderluh, Xanthine oxidase inhibitors beyond allopurinol and febuxostat; an overview and selection of potential leads based on in silico calculated physico-chemical properties, predicted pharmacokinetics and toxicity, Eur. J. Med. Chem. 135 (2017) 491−516.
[4] M.V. Rodrigues, A.F. Barbosa, J.F. da Silva, D.A. dos Santos, K.L. Vanzolini, M.C. de Moraes, A.G. Correa, Q.B. Cass, 9-Benzoyl 9-deazaguanines as potent xanthine oxidase inhibitors, Bioorg. Med. Chem. 24 (2016) 226−231.
[5] J.-M. Lü, Q. Yao, C. Chen, 3,4-Dihydroxy-5-nitrobenzaldehyde (DHNB) is a potent inhibitor of xanthine oxidase: a potential therapeutic agent for treatment of hyperuricemia and gout, Biochem. Pharmacol. 86 (2013) 1328−1337.
[6] H. Singh, S. Sharma, R. Ojha, M.K. Gupta, K. Nepali, P.M.S. Bedi, Synthesis and evaluation of naphthoflavones as a new class of non purine xanthine oxidase inhibitors, Bioorg. Med. Chem. Lett 24 (2014) 4192−4197.
[7] P. Pacher, Therapeutic effects of xanthine oxidase inhibitors: renaissance half a century after the discovery of allopurinol, Pharmacol. Rev. 58 (2006) 87−114.
[8] T. Hosoya, T. Sasaki, H. Hashimoto, R. Sakamoto, T. Ohashi, Clinical efficacy and safety of topiroxostat in Japanese male hyperuricemic patients with or without gout: an exploratory, phase 2a, multicentre, randomized, double-blind, placebo-controlled study, J. Clin. Pharm. Ther. 41 (2016) 298−305.
[9] C. B-Rao, A. Kulkarni-Almeida, K.V. Katkar, S. Khanna, U. Ghosh, A. Keche, P. Shah, A. Srivastava, V. Korde, K.V.S. Nemmani, N.J. Deshmukh, A. Dixit, M.K. Brahma, U. Bahirat, L. Doshi, R. Sharma, H. Sivaramakrishnan, Identification of novel isocytosine derivatives as xanthine oxidase inhibitors from a set of virtual screening hits, Bioorg. Med. Chem. 20 (2012) 2930−2939.
[10] S. Khanna, S. Burudkar, K. Bajaj, P. Shah, A. Keche, U. Ghosh, A. Desai, A. Srivastava, A. Kulkarni-Almeida, N.J. Deshmukh, A. Dixit, M.K. Brahma, U. Bahirat, L. Doshi, K.V.S. Nemmani, P. Tannu, A. Damre, C. B-Rao, R. Sharma, H. Sivaramakrishnan, Isocytosine-based inhibitors of xanthine oxidase: design, synthesis, SAR, PK and in vivo efficacy in rat model of hyperuricemia, Bioorg. Med. Chem. Lett 22 (2012) 7543−7546.
[11] K. Bajaj, S. Burudkar, P. Shah, A. Keche, U. Ghosh, P. Tannu, S. Khanna, A. Srivastava, N.J. Deshmukh, A. Dixit, Y. Ahire, A. Damre, K.V.S. Nemmani, A. Kulkarni-Almeida, C. B-Rao, R. Sharma, H. Sivaramakrishnan, Lead optimization of isocytosine-derived xanthine oxidase inhibitors, Bioorg. Med. Chem. Lett 23 (2013) 834−838.
[12] J. Evenäs, F. Edfeldt, M. Lepistö, N. Svitacheva, A. Synnergren, B. Lundquist, M. Gränse, A. Rönnholm, M. Varga, J. Wright, M. Wei, S. Yue, J. Wang, C. Li, X. Li, G. Chen, Y. Liao, G. Lv, A. Tjörnebo, F. Narjes, HTS followed by NMR based counterscreening. Discovery and optimization of pyrimidones as reversible and competitive inhibitors of xanthine oxidase, Bioorg. Med. Chem. Lett 24 (2014) 1315−1321.
[13] M. Kaur, A. Kaur, S. Mankotia, H. Singh, A. Singh, J.V. Singh, M.K. Gupta, S. Sharma, K. Nepali, P.M. Bedi, Synthesis, screening and docking of fused pyrano[3,2-d]pyrimidine derivatives as xanthine oxidase inhibitor, Eur. J. Med. Chem. 131 (2017) 14−28.
[14] J. Li, F. Wu, X. Liu, Y. Zou, H. Chen, Z. Li, L. Zhang, Synthesis and bioevaluation of 1-phenyl-pyrazole-4-carboxylic acid derivatives as potent xanthine oxidoreductase inhibitors, Eur. J. Med. Chem. 140 (2017) 20−30.
[15] X. Xu, L.M. Deng, L. Nie, Y.M. Chen, Y.Z. Liu, R.R. Xie, Z. Li, Discovery of 2-phenylthiazole-4-carboxylic acid, a novel and potent scaffold as xanthine oxidase inhibitors, Bioorg. Med. Chem. Lett 29 (2019) 525−528.
[16] A. Shi, L. Zhang, H. Wang, S. Wang, M. Yang, Q. Guan, K. Bao, W. Zhang, Design, synthesis and bioevaluation of 2-mercapto-6-phenylpyrimidine-4-carboxylic acid derivatives as potent xanthine oxidase inhibitors, Eur. J. Med. Chem.

155 (2018) 590–595.
[17] H.J. Tang, W. Li, M. Zhou, L.Y. Peng, J.X. Wang, J.H. Li, J. Chen, Design, synthesis and biological evaluation of novel xanthine oxidase inhibitors bearing a 2-arylbenzo[b]furan scaffold, Eur. J. Med. Chem. 151 (2018) 849–860.
[18] H.J. Tang, X.W. Zhang, L. Yang, W. Li, J.H. Li, J.X. Wang, J. Chen, Synthesis and evaluation of xanthine oxidase inhibitory and antioxidant activities of 2-arylbenzo[b]furan derivatives based on salvianolic acid C, Eur. J. Med. Chem. 124 (2016) 637–648.
[19] S.H. Nile, Y.S. Keum, A.S. Nile, S.S. Jalde, R.V. Patel, Antioxidant, anti-inflammatory, and enzyme inhibitory activity of natural plant flavonoids and their synthesized derivatives, J. Biochem. Mol. Toxicol. 32 (2018), e22002.
[20] M. de Araujo, Y.E.M. Franco, T.G. Alberto, M.C.F. Messias, C.W. Leme, A. Sawaya, P.O. Carvalho, Kinetic study on the inhibition of xanthine oxidase by acylated derivatives of flavonoids synthesised enzymatically, J. Enzym. Inhib. Med. Chem. 32 (2017) 978–985.
[21] Y. Li, C.M. Frenz, Z. Li, M. Chen, Y. Wang, F. Li, C. Luo, J. Sun, L. bohlin, Z. Li, H. Yang, C. Wang, Virtual and in vitro bioassay screening of phytochemical inhibitors from flavonoids and isoflavones against Xanthine oxidase and Cyclooxygenase-2 for gout treatment, Chem. Biol. Drug Des. 81 (2013) 537–544.
[22] M.D. Santi, M. Paulino Zunini, B. Vera, C. Bouzidi, V. Dumontet, A. Abin-Carriquiry, R. Grougnet, M.G. Ortega, Xanthine oxidase inhibitory activity of natural and hemisynthetic flavonoids from Gardenia oudiepe (Rubiaceae) in vitro and molecular docking studies, Eur. J. Med. Chem. 143 (2018) 577–582.
[23] E. Hofmann, J. Webster, T. Do, R. Kline, L. Snider, Q. Hauser, G. Higginbottom, A. Campbell, L. Ma, S. Paula, Hydroxylated chalcones with dual properties: xanthine oxidase inhibitors and radical scavengers, Bioorg. Med. Chem. 24 (2016) 578–587.
[24] R.M. Vitale, L. Antenucci, M. Gavagnin, G. Raimo, P. Amodeo, Structure-activity relationships of fraxamoside as an unusual xanthine oxidase inhibitor, J. Enzym. Inhib. Med. Chem. 32 (2017) 345–354.
[25] T.J. Zhang, S.Y. Li, W.Y. Yuan, Q.X. Wu, L. Wang, S. Yang, Q. Sun, F.H. Meng, Discovery and biological evaluation of some (1H-1,2,3-triazol-4-yl)methoxybenzaldehyde derivatives containing an anthraquinone moiety as potent xanthine oxidase inhibitors, Bioorg. Med. Chem. Lett 27 (2017) 729–732.
[26] T.J. Zhang, S.Y. Li, Y. Zhang, Q.X. Wu, F.H. Meng, Design, synthesis, and biological evaluation of 5-(4-(pyridin-4-yl)-1H-1,2,3-triazol-1-yl)benzonitrile derivatives as xanthine oxidase inhibitors, Chem. Biol. Drug Des. 91 (2018) 526–533.
[27] T.J. Zhang, S.Y. Li, W.Y. Yuan, Y. Zhang, F.H. Meng, Design, synthesis and molecular docking studies of N-(9,10-anthraquinone-2-carbonyl)amino acid derivatives as xanthine oxidase inhibitors, Chem. Biol. Drug Des. 91 (2018) 893–901.
[28] T. Zhang, Y. Lv, Y. Lei, D. Liu, Y. Feng, J. Zhao, S. Chen, F. Meng, S. Wang, Design, synthesis and biological evaluation of 1-hydroxy-2-phenyl-4-pyridyl-1H-imidazole derivatives as xanthine oxidase inhibitors, Eur. J. Med. Chem. 146 (2018) 668–677.
[29] T.J. Zhang, S.Y. Li, L. Wang, Q. Sun, Q.X. Wu, Y. Zhang, F.H. Meng, Design, synthesis and biological evaluation of N-(4-alkoxy-3-cyanophenyl)isonicotinamide/nicotinamide derivatives as novel xanthine oxidase inhibitors, Eur. J. Med. Chem. 141 (2017) 362–372.
[30] K. Matsumoto, K. Okamoto, N. Ashizawa, T. Nishino, FYX-051: a novel and potent hybrid-type inhibitor of xanthine oxidoreductase, J. Pharmacol. Exp. Ther. 336 (2010) 95–103.
[31] K. Okamoto, B.T. Eger, T. Nishino, S. Kondo, E.F. Pai, An Extremely Potent Inhibitor of Xanthine Oxidoreductase: crystal structure of the enzyme-inhibitor of complex and mechanism of inhibition, J. Biol. Chem. 278 (2002) 1848–1855.
[32] A. Fukunari, K. Okamoto, T. Nishino, B.T. Eger, E.F. Pai, M. Kamezawa, I. Yamada, N. Kato, Y-700 [1-[3-Cyano-4-(2,2-dimethylpropoxy)phenyl]-1H-pyrazole-4-carboxylic acid]: a potent xanthine oxidoreductase inhibitor with hepatic excretion, J. Pharmacol. Exp. Ther. 311 (2004) 519–528.
[33] K. Okamoto, K. Matsumoto, R. Hille, B.T. Eger, E.F. Pai, T. Nishino, The crystal structure of xanthine oxidoreductase during catalysis: implications for reaction mechanism and enzyme inhibition, Proc. Natl. Acad. Sci. 101 (2004) 7931–7936.
[34] E.A. Popova, A.V. Protas, R.E. Trifonov, Tetrazole derivatives as promising anticancer agents, Anti Cancer Agents Med. Chem. 17 (2018) 1856–1868.
[35] C. Gao, L. Chang, Z. Xu, X.F. Yan, C. Ding, F. Zhao, X. Wu, L.S. Feng, Recent advances of tetrazole derivatives as potential anti-tubercular and anti-malarial agents, Eur. J. Med. Chem. 163 (2019) 404–412.
[36] S.Q. Wang, Y.F. Wang, Z. Xu, Tetrazole hybrids and their antifungal activities, Eur. J. Med. Chem. 170 (2019) 225–234.
[37] J.U. Song, J.W. Jang, T.H. Kim, H. Park, W.S. Park, S.H. Jung, G.T. Kim, Structure-based design and biological evaluation of novel 2-(indol-2-yl) thiazole derivatives as xanthine oxidase inhibitors, Bioorg. Med. Chem. Lett 26 (2016) 950–954.
[38] J.U. Song, S.P. Choi, T.H. Kim, C.-K. Jung, J.-Y. Lee, S.-H. Jung, G.T. Kim, Design and synthesis of novel 2-(indol-5-yl)thiazole derivatives as xanthine oxidase inhibitors, Bioorg. Med. Chem. Lett 25 (2015) 1254–1258.
[39] S. Chen, T. Zhang, J. Wang, F. Wang, H. Niu, C. Wu, S. Wang, Synthesis and evaluation of 1-hydroxy/methoxy-4-methyl-2-phenyl-1H-imidazole-5-carboxylic acid derivatives as non-purine xanthine oxidase inhibitors, Eur. J. Med. Chem. 103 (2015) 343–353.
[40] Q. Guan, Z. Cheng, X. Ma, L. Wang, D. Feng, Y. Cui, K. Bao, L. Wu, W. Zhang, Synthesis and bioevaluation of 2-phenyl-4-methyl-1,3-selenazole-5-carboxylic acids as potent xanthine oxidase inhibitors, Eur. J. Med. Chem. 85 (2014) 508–516.
[41] S. Wang, J. Yan, J. Wang, J. Chen, T. Zhang, Y. Zhao, M. Xue, Synthesis of some 5-phenylisoxazole-3-carboxylic acid derivatives as potent xanthine oxidase inhibitors, Eur. J. Med. Chem. 45 (2010) 2663–2670.
[42] T.J. Zhang, Q.X. Wu, S.Y. Li, L. Wang, Q. Sun, Y. Zhang, F.H. Meng, H. Gao, Synthesis and evaluation of 1-phenyl-1H-1,2,3-triazole-4-carboxylic acid derivatives as xanthine oxidase inhibitors, Bioorg. Med. Chem. Lett 27 (2017) 3812–3816.
[43] E. Cristofer, T.E. Bryan, O. Ken, N. Tomoko, N. Takeshi, F.P. Emil, Crystal structures of bovine milk xanthine dehydrogenase and xanthine oxidase: structure-based mechanism of conversion, Proc. Natl. Acad. Sci. 97 (2000) 10723–10728.
[44] L. Kalé, R. Skeel, M. Bhandarkar, R. Brunner, A. Gursoy, N. Krawetz, J. Phillips, A. Shinozaki, K. Varadarajan, K. Schulten, NAMD2: greater scalability for parallel molecular dynamics, J. Comput. Phys. 151 (1999) 283–312.
[45] W. Humphrey, A. Dalke, K. Schulten, VMD: visual molecular dynamics, J. Mol. Graph. 14 (33–38) (1996) 27–38.
[46] S.H. Abbas, G.E.-D.A.A. Abuo-Rahma, M. Abdel-Aziz, O.M. Aly, E.A. Beshr, A.M. Gamal-Eldeen, Synthesis, cytotoxic activity, and tubulin polymerization inhibitory activity of new pyrrol-2(3H)-ones and pyridazin-3(2H)-ones, Bioorg. Chem. 66 (2016) 46–62.
[47] K. Vanommeslaeghe, E. Hatcher, C. Acharya, S. Kundu, S. Zhong, J. Shim, E. Darian, O. Guvench, P. Lopes, I. Vorobyov, A.D. Mackerell Jr., CHARMM general force field: a force field for drug-like molecules compatible with the CHARMM all-atom additive biological force fields, J. Comput. Chem. 31 (2010) 671–690.